

Infrared vibrational spectra of amorphous Si and Ge[†]

M. H. Brodsky and A. Lurio

IBM Thomas J. Watson Research Center, Yorktown Heights, New York 10598

(Received 10 September 1973)

We report the observation of the room-temperature infrared absorption spectrum of sputtered films of amorphous Si and Ge between 35 and 700 cm^{-1} . The spectra show a broad frequency range of absorption corresponding to the frequency range of the vibrational density of states in crystalline Si and Ge. We interpret the results in terms of a disorder-induced breakdown of the selection rules for vibronic infrared absorption in much the same way as occurs in Raman scattering. Discussion is given of related phenomena in alloys and neutron-irradiated crystals.

I. INTRODUCTION

Crystalline Si and Ge have no first-order infrared (ir) absorption because of the symmetry of their lattice. Some second-order absorptions are allowed and are observed as weak ir absorption bands having peak absorption constants of 13 and 30 cm^{-1} at frequencies of 610 and 345 cm^{-1} for Si and Ge, respectively.¹ In amorphous Si and Ge (*a*-Si and *a*-Ge), however, the lack of long-range order relaxes the crystal momentum and symmetry rules prohibiting first-order absorption, and, in principle, all vibrational modes can contribute to first-order absorption processes. We report the observation and interpretation of the first-order vibrational spectra of *a*-Si and *a*-Ge. The spectra and their interpretation are similar to that reported from Raman scattering studies on the same materials.² The essential result is that the basic features of a suitably weighted and broadened version of the crystalline vibrational density of states are observed in the corresponding amorphous absorption spectrum.

Previous work by Tauc *et al.*³ indicated an absorption peak near 270 cm^{-1} in *a*-Ge. They speculated that it was due to the disorder-induced zone-center TO phonon. Recently, Prettl *et al.*⁴ have reported similar results. Our results show absorption in addition to the 270- cm^{-1} peak and we give a more general interpretation to the results. Stimets *et al.*⁵ have reported *a*-Ge spectra similar to ours. We are aware of no previous measurements for *a*-Si. There exists a large literature of ir absorption studies on neutron-damaged crystalline Si and Ge.⁶ Some of these studies show absorption spectra qualitatively consistent with ours, but with smaller absorption constants. We offer the interpretation that such spectra arise from small regions of amorphous material dispersed throughout the crystals.

II. EXPERIMENTAL PROCEDURES

The *a*-Si and *a*-Ge films used in this experiment were prepared by rf sputtering of nominally undoped material in an argon atmosphere. The sput-

tering chamber was pre-evacuated to less than 10^{-7} torr before backfilling with argon. The pumping apparatus consisted of oil-diffusion, cryogenic, and titanium-sublimation pumps. Each *a*-Si film was examined for the presence of bonded oxygen by searching for the Si-O-Si absorption band near 1100 cm^{-1} . We found no absorption in this region for the films reported here. Assuming a peak absorption constant⁷ of 1 cm^{-1} for an oxygen concentration of $5 \times 10^{17} \text{ cm}^{-3}$, we estimate that our samples contained less than 0.2% bonded oxygen. Some of our early films did show absorption near 1100 cm^{-1} and this led us to require stringent cleanliness procedures in our sputtering process. We have no definitive information on the question of a possible oxygen-related absorption in *a*-Ge.

All the films used in obtaining the data reported here were deposited on high purity ($>100 \Omega \text{ cm}$) oxygen-free single-crystal Si substrates. The substrates were 2.5 cm in diameter and were wedged in thickness from 0.02 to 0.03 cm across the face of the sample. The wedge configuration eliminated the complication of multiple-internal-reflection interference effects in the substrate. Each substrate was coated with *a*-Si or *a*-Ge on both sides to increase the available optical-absorption path length. The coatings were alternately placed first on one side then the other, then again on the first side and so on until four to six layers were built up. We found the alternate layering procedure necessary to reduce the accumulated strain. The strain which developed during a single deposition were sometimes enough to crack our films and/or substrates for film thickness greater than about 6 μm . By the above procedure we were occasionally able to prepare amorphous samples as thick as 35 μm .

The transmission spectra were obtained at room temperature in a Perkin-Elmer Model 301 far-infrared spectrometer. Representative spectra were checked by reproducing the results in a Beckman IR-11 spectrophotometer. Data were taken in both single-beam and double-beam modes. The sample spectra were recorded relative to the transmission of an uncoated matched substrate.

III. DATA REDUCTION AND RESULTS

Shown in Figs. 1 and 2 are the measured transmission versus frequency (in wave numbers) for multiple layers of α -Si and α -Ge films. Both curves are for amorphous films on wedged single-crystal silicon substrates relative to an uncoated substrate. From this data and the total thickness of the films we can obtain $\alpha(\nu)$, the absorption coefficient, as a function of frequency ν .

We have estimated the film thickness in two ways: (i) from Tallysurf measurements on partially masked substrates sputtered simultaneously with each coating of the measured sample and (ii) from near infrared interference oscillations within the film. As mentioned previously, no oscillations arise from the substrates because they are wedges. Neither of these measurements is probably more accurate than $\pm 20\%$. The Tallysurf measurements were carried out on a film sputtered adjacent to but not in the identical location of the sample. We have observed variations in sputtered thicknesses as large as $\pm 20\%$ over the region of the sputtering cathode. Thickness determinations from interference oscillations in the films require knowledge of the film index of refraction. It is well known that for α -Si and α -Ge, properties such as the index of refraction are strongly dependent on preparation conditions and variations of $\pm 10\%$ to 20% are not uncommon.⁸ Furthermore, beats can occur between the different thickness films on either side of the substrate. For the films used in obtaining the data shown in Figs. 1 and 2 we estimate the total α -Si and α -Ge thicknesses to be 37 ± 4 and 25 ± 3 μm , respectively.

Let us consider the α -Si data first. Since the index of refraction of α -Si can be approximately 3.6, while that of crystalline Si is 3.4, the reflection coefficient at the α -Si to Si interface in such a case would only be 0.03. If our films do have these or similar parameters, then, to within the preci-

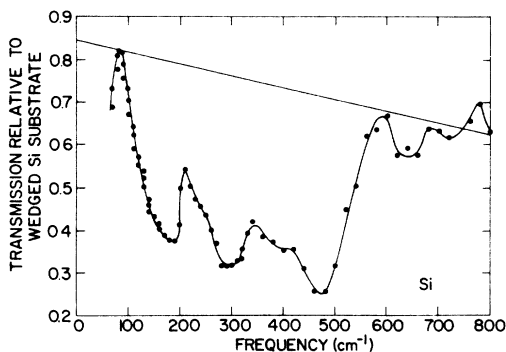


FIG. 1. Transmittance of $37 \mu\text{m}$ of α -Si on both sides of a wedged high-resistivity crystalline Si substrate relative to a matched uncoated substrate.

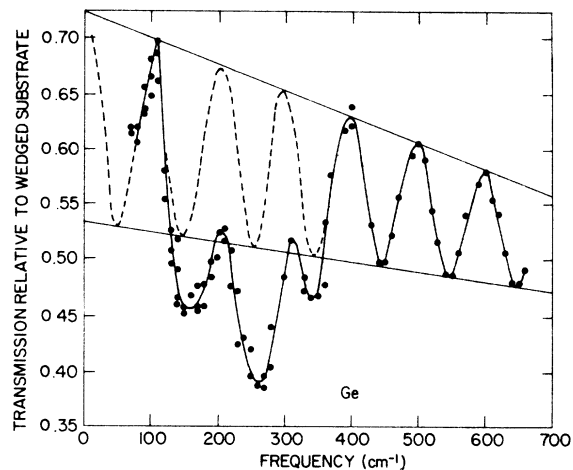


FIG. 2. Transmittance of $25 \mu\text{m}$ of α -Ge on both sides of a wedged high-resistivity crystalline Si substrate relative to a matched uncoated substrate.

sion of the present results, we can ignore any interference oscillations. Inhomogeneously thick films would also have washed out interference fringes. The data of Fig. 1 is for such a film. This means that the data of Fig. 1 is just the transmission coefficient of the film alone. The straight line drawn across the top of the curve is the line representing zero loss. This is a simpler special case of Eq. (1), described below. The fact that it does not go to 100% at zero frequency is probably due to surface roughness. Figure 3 shows the absorption coefficient α versus frequency for α -Si at room temperature. $\alpha(\nu)$ is obtained from the transmission $T(\nu)$ by the relation $T(\nu) = e^{-\alpha(\nu)d}$, where d is the total film thickness and the 100% transmission line is taken to be the straight line drawn across the top in Fig. 1.

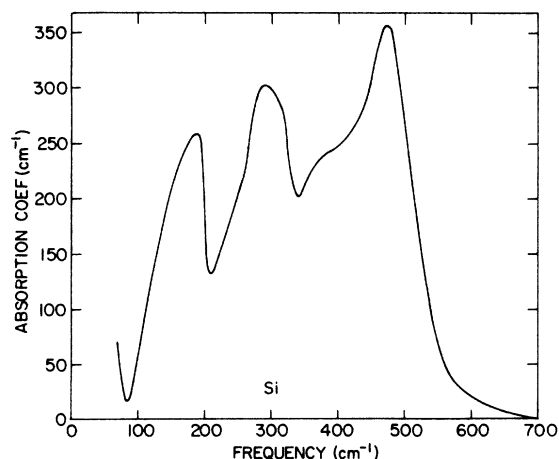


FIG. 3. Absorption coefficient of α -Si vs frequency expressed in wave numbers (cm^{-1}).

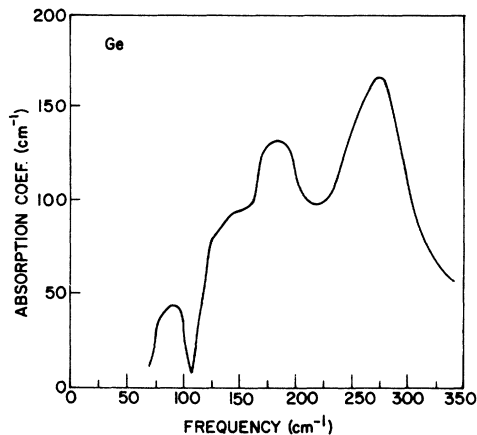


FIG. 4. Absorption coefficient of α -Ge vs frequency expressed in wave numbers (cm^{-1}).

The transmission data for α -Ge (Fig. 2) clearly shows the interference oscillations in the α -Ge film. We use the following empirical curve-fitting procedure to subtract the background. As shown in the Appendix, the transmitted intensity oscillations should be approximately given by an expression of the form

$$T = Ae^{-C\nu} / (1 - Be^{-C\nu/2} \cos 4\pi\nu nd), \quad (1)$$

where ν is the frequency in wave numbers and A , B , and C are constants. By fitting our experimental curve in the region 400 – 650 cm^{-1} , we find $C = 4.39 \times 10^{-4} \text{ cm}$, $A = 0.677$, $B = 0.105$, and $nd = 5.03 \times 10^{-3} \text{ cm}$. In this fit we have assumed the same thickness on both sides of the substrate, since no beats between the two films were seen. In other samples beats have occurred. The weak absorption in the region outside of the amorphous absorption region can be ascribed to surface irregularity and film granularity. The dotted line in Fig. 2 is the extension of Eq. (1) into the region of strong absorption. The line given by Eq. (1) is taken to be the 100% transmission line, and the absorption coefficient $\alpha(\nu)$ is calculated as in the silicon case. In Fig. 4 the absorption coefficient α versus frequency is plotted for our room-temperature α -Ge data.

TABLE I. The strengths of the disordered-induced infrared absorption in α -Si and α -Ge are shown in terms of the contributions Δn and $\Delta\epsilon$ to the index of refraction n and dielectric constant ϵ . The ranges of integration of Eq. (2) are also shown.

	Range of integration	n	Δn	ϵ	$\Delta\epsilon$
α -Si	85 – 600 cm^{-1}	3.6	0.07	13.0	0.5
α -Ge	70 – 360 cm^{-1}	4.2	0.04	17.6	0.3

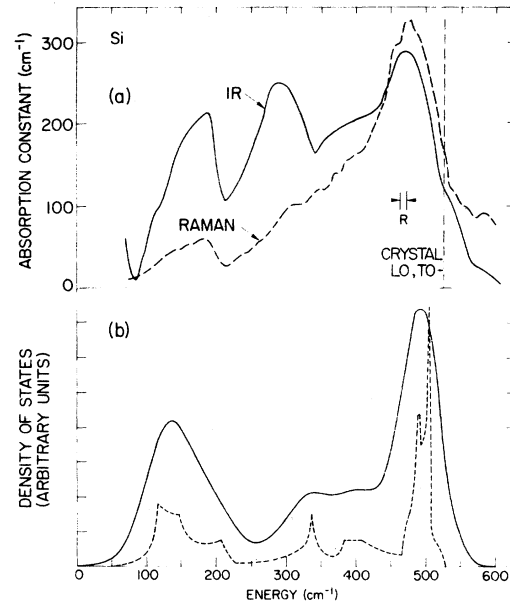


FIG. 5. (a) Room-temperature infrared absorption constant (solid line) vs wave number for amorphous Si. Also shown for comparison is the reduced Raman spectrum (dashed line) from the room-temperature data of Ref. 2. (b) Density of states (dashed line) of crystal Si from a fit (Ref. 12) to neutron scattering data. The solid line is the broadened density of states.

It is useful to estimate the integrated absorption strengths in terms of the contribution made to the dielectric constant by the disordered induced absorption bands of Figs. 3 and 4. We note that the change in the index of refraction between the low- and high-frequency sides of an absorption band is given by⁹

$$\Delta n = \frac{1}{2\pi^2} \int_{\text{low}}^{\text{high}} \frac{\alpha}{\nu^2} d\nu. \quad (2)$$

It follows that the change in the dielectric constant ϵ across the absorption region is

$$\Delta\epsilon = 2n\Delta n + \Delta n^2. \quad (3)$$

For α -Si¹⁰ and α -Ge¹¹ sputtered at room temperature, the values of n are approximately equal to 3.6 and 4.2, respectively. Although there is considerable uncertainty,^{8,10,11} of order 10%, in these values, they are known well enough for us to use them to estimate $\Delta\epsilon$ as shown in Table I.

IV. DISCUSSION OF RESULTS

Figure 5 shows four Si spectra for comparison. The solid curve in Fig. 5(a) is our room-temperature infrared absorption spectrum for α -Si. The dashed curve in Fig. 5(a) is the corresponding reduced Raman spectrum obtained by Smith *et al.*² From Fig. 5(a), we note some qualitative similarities between the two spectra; however, there are

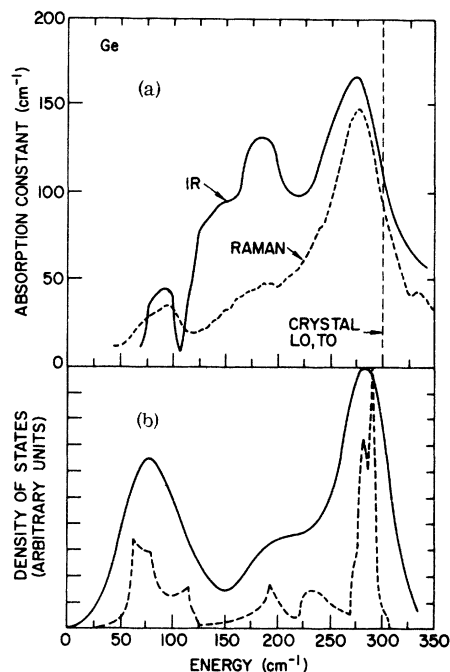


FIG. 6. (a) Room-temperature infrared absorption constant (solid line) vs wave number for amorphous Ge. Also shown for comparison is the reduced Raman spectrum (dashed line) from the room-temperature data of Ref. 13. (b) Density of states (dashed line) of crystal Ge from a fit (Ref. 12) to neutron scattering data. The solid line is the broadened density of states.

some important differences. Most striking is the greater clarity and enhanced strength of the lower frequency spectral features in the ir results.

Following Smith *et al.*,² we also compare our results with the crystalline phonon density of states. The dashed curve in Fig. 5(b) is the phonon density of states for crystal Si as obtained by Dolling and Cowley.¹² Dolling and Cowley used an eleven-parameter dipole-approximation model to interpolate between the dispersion curves measured by neutron inelastic scattering. The smooth curve of Fig. 5(b) is a Gaussian-broadened version of the crystal density of states. We used the same Gaussian broadening as described in Ref. 2. Figure 6 shows the equivalent results for Ge.¹³

It is apparent from Figs. 5 and 6 that there is some relation between the ir absorption (or Raman scattering) and the entire crystalline vibrational densities of states. This is in contrast to the typical crystalline case where only a few special (if any) vibrations of suitable momenta and symmetry are ir or Raman active. To make this qualitative observation more meaningful requires a two-step argument. First, one must really determine the amorphous densities of states rather than just use an *ad hoc* broadening of the crystalline densities, as is done here and in Refs. 2 and 13. Because

the short-range order is essentially the same in both cases, there are good reasons to believe that the amorphous and crystalline densities of states are in fact similar. A quantitative calculation for some simple models of a tetrahedrally bonded amorphous semiconductor has been given by Alben *et al.*,¹⁴ and their results show that the broadening procedure we use is reasonable as long as only the gross features are of interest. The physical reason for this is that the crystalline densities of states for Si and Ge are generally well represented by a short-range-force model that can be easily carried over to the amorphous forms. There are important aspects of the density-of-states spectra that depend on long-range order, but to first approximation these can be ignored.

The second step of the argument is to say to what extent the matrix-element effects for ir absorption (or Raman scattering) alter or distort the shape of the density-of-states curve when measured by an ir (or Raman) experiment. We see in Figs. 5(a) and 6(a) that there are differences between the ir and Raman spectra so that there definitely are some matrix-element effects. Alben *et al.*,¹⁴ have also shown how these differences can be accounted for within the context of a simple disordered-network-model representation of the amorphous state in terms of distortions in the tetrahedral arrangement of atoms. For the ir absorption, the model uses the simplest form of a disordered-induced frequency-dependent dipole moment in terms of motions of the bond charges of triads of atoms. In this model the dipole moments of the bond charges all cancel each other out to net zero contribution in the crystalline case of perfect tetrahedral symmetry, as they must, for we know crystalline Si and Ge have no allowed first-order absorption. The Raman activity, however, differs in that it is composed of a part that is symmetry allowed in the crystals and an additional part owing to the less than perfect tetrahedral arrangements of the atoms in the model. It follows that the Raman spectrum has relatively more strength in the region of allowed crystalline processes and the ir absorption strength is more nearly evenly weighted across the vibrational spectrum. This is in accord with the spectra of Figs. 5(a) and 6(a). Prettl *et al.*,⁴ have given another argument for the differences between the ir and Raman couplings as a function of the vibrational energy. Prettl *et al.*,⁴ predict an enhancement of the low-frequency region of the Raman spectra relative to the infrared spectra. This is opposite to what we show in Figs. 5 and 6. We feel their argument is not convincing because they equate energy dependence with momentum dependence over the entire spectrum, which is a reasonable approximation only in the long-wavelength low-frequency region of the dis-

persion curves, but not a very good approximation over most of the vibrational spectrum.

We point out that the integrated absorption strengths as expressed in terms of the contribution to the dielectric constant (see Table I) are about 0.5 for α -Si and 0.3 for α -Ge. This compares with a typical value of 2 for a related polar III-V semiconductor crystal such as GaAs. Thus, the total vibronic absorption induced by the disorder in homopolar Si and Ge is within an order of magnitude of the strong polar absorptions in the crystalline III-V's. We know of no theory which quantitatively predicts the absorption strength.

The strength of this absorption leads us to believe that previous workers have seen similar effects in neutron-damaged crystalline Si and Ge. If a small percentage of the crystal were converted to amorphous material in the tracks of the neutrons,¹⁵ then it is reasonable to expect an observable infrared absorption from the dispersed amorphous regions. We have put some Si and Ge single-crystal wafers in a neutron pile, and have observed ir spectra similar to Figs. 3 and 4 but with considerably reduced values of α . This is not a new result, but merely a repetition of the many previous studies on irradiated crystals.⁶ What we do offer is the interpretation that these neutron-induced spectra are really a disordered-induced phenomenon related to the amorphous case.

Similar disordered-induced ir effects have been seen in still another type of system, namely, $\text{Ge}_x\text{Si}_{1-x}$ crystalline alloys. For small values of x a spectrum qualitatively similar to the α -Si spectrum is seen, and for x near 1 a spectrum similar to the α -Ge spectrum is seen.¹⁶

SUMMARY

We have reported results for the far-infrared absorption spectra of α -Si and α -Ge. The absorption spectra are interpreted as the disordered-induced ir activity of the vibrational density of states with an absorption strength only a little weaker than that of related polar materials.

ACKNOWLEDGMENTS

We thank J. Cuomo for advice and guidance in the preparation of the samples, V. Richardson for the operation of sputtering apparatus, L. Manganaro for his assistance in the data acquisition, J. Philbrick for the use of his spectrophotometer, and Dr. R. Alben, Dr. J. E. Smith, Jr., and Dr. F. Stern for useful discussions.

APPENDIX

In this Appendix we calculate an expression for the transmissivity through a wedged transparent substrate having a lossy amorphous film on either side of the substrate. We assume that the films are of uniform thickness so that we must take account of phase relations in the multiple reflections from each boundary of the film. For the wedged substrate, because of the wedging, phases may be neglected and we need add only intensities in the multiple reflections from each substrate boundary. Born and Wolf¹⁷ have shown that for normal incidence the transmissivity and reflectivity of a film of index n_2 for light incident from a region of index n_1 into a region of index n_3 is given by

$$R_{13} = \left| \frac{\hat{r}_{12} + \hat{r}_{23} e^{-2(\gamma_2 - i\beta_2)}}{1 + \hat{r}_{12} \hat{r}_{23} e^{-2(\gamma_2 - i\beta_2)}} \right|^2 = \frac{r_{12}^2 + r_{23}^2 e^{-4\gamma_2} + 2r_{12} r_{23} e^{-2\gamma_2} \cos(2\beta_2 - \phi_{12} + \phi_{13})}{1 + r_{12}^2 r_{23}^2 e^{-4\gamma_2} + 2r_{12} r_{23} e^{-2\gamma_2} \cos(2\beta_2 + \phi_{12} + \phi_{23})},$$

(R_{31} is different from R_{13} and is obtained by interchanging all the indices one and three in the expression for R_{13}), and

$$T_{13} = \frac{n_3}{n_1} \left| \frac{\hat{t}_{12} \hat{t}_{23} e^{-(\gamma_2 - i\beta_2)}}{1 + \hat{r}_{12} \hat{r}_{23} e^{-2(\gamma_2 - i\beta_2)}} \right|^2 = \frac{(n_3/n_1) t_{12}^2 t_{23}^2 e^{-2\gamma_2}}{1 + r_{12}^2 r_{23}^2 e^{-4\gamma_2} + 2r_{12} r_{23} e^{-2\gamma_2} \cos(2\beta_2 + \phi_{12} + \phi_{23})}$$

where

$$\hat{r}_{ij} = (\hat{n}_i - \hat{n}_j) / (\hat{n}_i + \hat{n}_j) = -\hat{r}_{ji} = r_{ij} e^{i\phi_{ij}},$$

$$\hat{t}_{ij} = 2\hat{n}_i / (\hat{n}_i + \hat{n}_j),$$

$$\beta_2 + i\gamma_2 = (2\pi/\lambda_0) \hat{n}_2 d,$$

$$\tan \phi_{ij} = \text{Im}(\hat{r}_{ij}) / \text{Re}(\hat{r}_{ij}).$$

β_2 and γ_2 are real, λ_0 is the vacuum wavelength of the light, d is the film thickness, and \hat{n}_i is the complex index of refraction. Only for the amorphous film is it necessary to consider the complex

part of \hat{n}_i . Experimentally, it is found that $\text{Im} \hat{n}_2 / \text{Re} \hat{n}_2 \leq 0.005$, so \hat{r}_{ij} can be taken as real in all the above expressions with negligible error. The quantity γ_2 , however, is not negligible and must be retained in the exponential. Taking \hat{r}_{ij} as real yields the simplification

$$\frac{n_3}{n_1} = \frac{1 + r_{12}}{1 - r_{12}} \frac{1 + r_{23}}{1 - r_{23}},$$

and also permits us to drop ϕ_{12} and ϕ_{13} and rewrite T_{13} as

$$T_{13} = T_{31} = \frac{(1 - r_{12})^2 (1 - r_{23}^2) e^{-2\gamma_2}}{1 + r_{12}^2 r_{23}^2 e^{-4\gamma_2} + 2r_{12} r_{23} e^{-2\gamma_2} \cos 2\beta_2}$$

For the multiple reflections from each boundary of the substrate, the effect of the films is taken into account by using the R and T derived above for the reflection and transmission coefficient at each substrate boundary. We will replace the subscripts 1, 2, and 3 by A , G , or S standing for air,

germanium, or silicon. Superscripts 1 and 2 will be used to denote the film on the incident light and transmitted light sides, respectively. With this notation we find for the total transmitted intensity:

$$T = T_{AS}^{(1)} T_{SA}^{(2)} / (1 - R_{SA}^{(1)} R_{SA}^{(2)}),$$

which becomes

$$T = (1 - r_{AG}^2 - r_{GS}^2) e^{-2(\gamma+2)} \{ [1 - (r_{SG}^2 + r_{AG}^2 e^{-4\gamma_1}) (r_{SG}^2 + r_{GA}^2 e^{-4\gamma_2})] + 2r_{AG} r_{GS} [(1 - r_{SG}^2 - r_{GA}^2 e^{-4\gamma_2}) e^{-2\gamma_1} \times \cos 2\beta_1 + (1 - r_{SG}^2 - r_{GA}^2 e^{-4\gamma_1}) e^{-2\gamma_2} \cos 2\beta_2] \}^{-1}.$$

It is justified to neglect $r_{SG} \approx 0.011$ compared to $r_{GA} \approx 0.378$. In addition, we will take the case of equal film thicknesses on both sides of the substrate. Then T reduces to

$$T = \frac{(1 - r_{AG}^2)^2 e^{-4\gamma}}{1 - r_{AG}^4 e^{-8\gamma} + 4r_{AG} r_{GS} (1 - r_{GA}^2 e^{-4\gamma} e^{-2\gamma}) \cos 2\beta}$$

where $\gamma = \gamma_1 = \gamma_2$ and $\beta = \beta_1 = \beta_2$. This we will approximate by

$$T = A e^{-4\gamma} / (1 - B e^{-2\gamma} \cos 2\beta).$$

Since $r_{AG} r_{GS}$ is negative, we have used a minus sign before B so that B is a positive constant.

[†]A preliminary oral version of this paper was given at the March, 1972 American Physical Society meeting; see A. Lurio and M. H. Brodsky, *Bull. Am. Phys. Soc.* **17**, 322 (1972).

¹W. G. Spitzer, in *Semiconductors and Semimetals*, edited by R. K. Willardson and A. C. Beer (Academic, New York, 1967), Vol. 3, p. 17.

²J. E. Smith, Jr., M. H. Brodsky, B. L. Crowder, M. I. Nathan, and A. Pinczuk, *Phys. Rev. Lett.* **26**, 642 (1971).

³J. Tauc, A. Abraham, R. Zallen, and M. Slade, *J. Non-Cryst. Solids* **4**, 279 (1970).

⁴W. Prettl, M. J. Shevchik, and M. Cardona, *Phys. Status Solidi B* **59**, 241 (1973).

⁵R. W. Stimets, J. Waldman, J. Lin, T. S. Chang, R. J. Temkin, and G. A. N. Connell, *Solid State Commun.* **13**, 1485 (1973).

⁶H. Y. Fan and A. K. Ramadas, *J. Appl. Phys.* **30**, 1127 (1959); M. Balkanski and W. Mazerewics, *J. Phys. Chem. Solids* **23**, 573 (1962); J. F. Angress, T. Arai, A. R. Goodwin, and S. D. Smith, in *Proceedings of the Seventh International Conference on the Physics of Semiconductors, Paris*, 1964, edited by M. Hulin (Academic, New York, 1964), p. 1116.

⁷W. Kaiser and P. H. Keck, *J. Appl. Phys.* **28**, 882 (1957).

⁸M. H. Brodsky, *J. Vac. Sci. and Tech.* **8**, 125 (1971).

⁹T. S. Moss, *Optical Properties of Semiconductors* (Academic, New York, 1959), p. 27.

¹⁰M. H. Brodsky, R. S. Title, K. Weiser, and G. D. Pettit, *Phys. Rev. B* **1**, 2632 (1970).

¹¹G. A. N. Connell, R. J. Temkin, and W. Paul, *Adv. Phys.* (to be published).

¹²G. Dolling and R. A. Cowley, *Proc. Phys. Soc. Lond.* **88**, 463 (1966).

¹³J. E. Smith, Jr., M. H. Brodsky, B. L. Crowder, and M. I. Nathan, in *Proceedings of the Second International Conference on Light Scattering in Solids*, edited by M. Balkanski (Flammarion, Paris, 1971), p. 330.

¹⁴R. Alben, J. E. Smith, Jr., M. H. Brodsky, and D. Weaire, *Phys. Rev. Lett.* **30**, 1141 (1973); and *Proceedings of the Fifth International Conference on Liquid and Amorphous Semiconductors* (to be published).

¹⁵F. L. Vook and H. J. Stein, *Radiat. Eff.* **2**, 23 (1969).

¹⁶A. E. Cosand and W. G. Spitzer, *J. Appl. Phys.* **42**, 5241 (1971).

¹⁷M. Born and E. Wolf, *Principles of Optics* (Pergamon, New York, 1959), Chaps. 1 and 13.